PRAMANA
— journal of
physics

Vol. 47, No. 4,
October 1996
pp. 283–307

Nonlinear travelling waves in ϕ^6 polarizable model

NABONITA D CHOWDHURY* and SANKAR P SANYAL[†]
Department of Physics, Barkatullah University, Bhopal 462026 India
*Present Address: School of Physical Sciences, Jawaharlal Nehru University, New Delhi 110067, India
[†]Author for correspondence
[†]Present Address: Forschung Zentrum Karlsruhe Institut für Nukleare Festkorper-Physik, PB 3640, Karlsruhe, Germany

MS received 10 August 1994; revised 5 August 1995

Abstract. We present a complete theoretical analysis of the periodic and non-periodic travelling waves in a diatomic chain model, in the continuum limit by incorporating nonlinear sixth order polarization potential (ϕ^6) at the anion site. We have formulated a nonlinear lattice dynamical theory in which various energy curves are obtained for different types and magnitudes of the core-shell force constants. For periodic solutions, we have obtained two types of commensurate wave amplitudes which propagate in the opposite direction with respect to each other. For nonperiodic solutions, we have obtained various travelling excitations such as kink, antikink, excitons etc. for different values of the mass ratio and velocity parameter. The dipole moment per unit charge for $SrTiO_3$ has been calculated and it is found that the nonlinear excitations in this model carry large amount of energy as compared to those obtained from harmonic and anharmonic optical phonons in the ϕ^4-polarizable model.

Keywords. Nonlinear dynamics; phase transition.

PACS No. 77·80

1. Introduction

The nonlinear excitations play a dominant role in the dynamical properties of condensed matter systems [1–4]. These excitations are of great importance as they carry large amount of energy in various systems of solids such as photo-ferroelectrics [5] and biomolecules [1]. These type of excitations are obtained from large amplitude solutions which do not obey the principle of superposition. Various types of nonlinear excitations known so far are kinks, periodons and excitons. The kink solution corresponds to finite energy transition from one stable homogenous state (i.e., ferroelectric state) to another, where the time varies from $-\infty$ to ∞. Kink excitation with metastable instantaneous behaviour are called excitons. Periodons are known as nonlinear periodic waves with subharmonic scaling by 3, which locally show the character of excitons but is globally that of phonons.

The nonlinear excitations show their existence in various low dimensional systems and have their connection with the "central peak" phenomena observed in the ferroelectric materials near the structural phase transition [6]. From the theoretical point of view, Behera and Khare [7] suggested that kinks as well as excitons contribute to the formation of the central peak. Periodons play a role in photo induced effects in ferroelectrics, which suggests their applications to biological systems where nonlinear and nearly loss-free cooperative phenomena such as "active transport" are understood [5]. For the description of the nonlinear dynamical properties of ferroelectrics, a simple diatomic shell model was introduced [2], in terms of strongly anisotropic polarizability of the oxygen and chalcogenide ions which experience a configurationally unstable nonlinear electron-phonon interactions between its core and shell. In the self-consistent phonon approximation, the dynamical properties like soft mode, dielectric constant and phonon dispersion curves are fairly described well in the ϕ^4-polarizability model [1–3]. In one-dimensional picture, exact nonlinear solutions are obtained by Buttner and Bilz [3]. They have also obtained nonlinear periodic solutions (periodons), in addition to the static solutions of kink type. Exact nonlinear travelling wave solutions in the continuum limit are obtained in the ferroelectrics by Benedek *et al* [4]. They have solved the equation of motion of a diatomic chain, considering fourth order (ϕ^4) on-site polarization potential at anion and found the existence of kinks and domain walls. This type of analysis of the travelling wave solutions in the continuum limit helps in the understanding of the nonlinear periodic and nonperiodic excitations.

In the present paper we intend to present the classification and analysis of the travelling wave solutions in a diatomic lattice, in the continuum limit for an anharmonic sixth order polarization potential (ϕ^6) at the anion site. The present work is highly motivated by the experimental facts on certain optical crystals. Adair *et al* [8] have experimentally measured the nonlinear refractive indices in a large number of optical crystals by using the technique of nearly degenerate three wave mixing. The nonlinear refractive index in a crystal arises from the contributions of intraionic and interionic nonlinear polarizations, which gives a very high value of nonlinear dipole moment. For ferroelectric system i.e., $SrTiO_3$, they have measured the nonlinear refractive index as $26{\cdot}7(10^{-19}\,\mathrm{esu})$ which is a very large value as compared to linear index data i.e., $2{\cdot}31(1{\cdot}06\,\mu\mathrm{m})$. The hyperpolarizability of oxygen ion is responsible for high value of refractive index. We have used the ϕ^6 polarizable potential to understand the high value of refractive indices in ferroelectrics, in terms of the nonlinear travelling waves.

We have considered a model of the one-dimensional diatomic lattice with harmonic coupling between neighbouring sites and anharmonic on-site potential at the polarizable ion as [9]

$$V_{\mathrm{p}}(w_{1,n}) = \sum_n \left[\tfrac{1}{2} g_2 w_{1,n}^2 + \frac{1}{m+2} g_4 w_{1,n}^{m+2} + \frac{1}{2m+2} g_6 w_{1,n}^{2m+2} \right] \tag{1}$$

with $m = 2$. We have started our analytical analysis by first calculating the potential energy of the anharmonic oscillator at the turning point w_0 for different choices of core-shell force constants i.e., (I) $g_2 > 0$, $g_4 > 0$, $g_6 > 0$ (II) $g_2 < 0$, $g_6 < 0$, $g_4 > 0$ (III) $g_2 > 0, g_6 > 0, g_4 < 0$ for $g_2 <, > 2f$ and $g_4^2 >, =, < 4g_2 g_6$. By noticing the variation of energy with displacement coordinate under the conditions mentioned above, we select only case (II) i.e., $g_2 < 2f$ and $g_4^2 = 4g_2 g_6$ for investigating the travelling wave. This potential in case (II) leads to negative value for large $w_{1,n}$, but the harmonic intra-site potential of the diatomic lattice (V_{L}) stabilizes the potential $V_{\mathrm{p}}(w_{1,n})$. The total potential is the sum of polarization (on-site) (V_{p}) and harmonic (intra-site) (V_{L}) potential, which now have a finite energy solution and remain valid for all the conditions. In this case, the energy structure develops a double well, similar to the double well obtained in ϕ^4 model for $g_2 < 0$ and $g_4 > 0$. The only difference arise at the minima position where the energy remains degenerate for three displacements which are close to each other. Hence the present case is a modified ferroelectric case with minima at the displacement $(-g_4/2g_6)^{1/2}$ which is equivalent to $(-g_2/g_4)^{1/2}$, by using the approximation $g_4^2 = 4g_2g_6$. The minima under this approximation reduces to $\sqrt{2}$ times the minima of ϕ^4 potential. This case now corresponds to second order phase transition. The present case discussed is a special case of ϕ^6 polarizable model. We have further, analyzed the periodic and non-periodic travelling wave solutions and obtained kink and antikink solutions, which were not obtained in Benedek's treatment. We have also calculated the dipole moment per unit charge carried by the nonlinear excitations for $SrTiO_3$.

2. Theory

The starting point of the present theory is basically to consider the higher order (i.e. sixth) polarization potential at the site of an anion in a one-dimensional diatomic lattice with nearest and next nearest neighbour interactions (see figure 1). The Hamiltonian can be expressed as

$$H = T + V_L + V_p(w_{1,n}), \tag{2}$$

where

$$T = \tfrac{1}{2}\sum_n [m_1 \dot{u}_{1,n}^2 + m_2 \dot{u}_{2,n}^2 + m_e \dot{v}_{1,n}^2] \tag{3}$$

and

$$\begin{aligned} V_L = \tfrac{1}{2}\sum_n [&f'(u_{1,n+1} - u_{1,n})^2 + f'(u_{1,n-1} - u_{1,n})^2 + f(u_{2,n} - v_{1,n})^2 \\ &+ f(u_{2,n} - v_{1,n-1})^2 + f(u_{2,n} - v_{1,n+1})^2 + f(u_{2,n-1} - v_{1,n})^2 \\ &+ f(u_{2,n-1} - v_{1,n-1})^2]. \end{aligned} \tag{4}$$

Here $u_{1,n}$ and $u_{2,n}$ are the displacements of the core of anion (1) and cation (2) in the nth cell. The respective masses of the ions 1 and 2 are m_1, m_2 and m_e is the mass of the electron shell of anion, which has displacement $v_{1,n}$. f is the nearest neighbour force constant between two ions in the nth cell. f' is the core-core force constant of the anion in two adjacent cells $(n, n \pm 1)$. g_2, g_4 and g_6 are the second, fourth and sixth order anharmonic core-shell force constants. By defining a relative core-shell displacement coordinate of the polarizable ion as $w_{1,n} = v_{1,n} - u_{1,n}$, and using adiabatic approximation $(m_e \sim 0)$, we have obtained a nonlinear second order differential equation of motion in relative core-shell coordinate $w_{1,n}$ as

$$\begin{aligned} &(\alpha + \delta w_{1,n}^2 + \gamma w_{1,n}^4)\ddot{w}_{1,n} + 2\delta w_{1,n}\dot{w}_{1,n}^2 + 4\gamma w_{1,n}^3 \dot{w}_{1,n}^2 \\ &+ \frac{2f}{\mu}(g_2 w_{1,n} + g_4 w_{1,n}^3 + g_6 w_{1,n}^5) - f\left(\frac{f}{m_2} - \frac{2f'}{m_1}\right)(u_{1,n+1} + u_{1,n-1} - 2u_{1,n}) \\ &- \frac{f^2}{m_2}(w_{1,n+1} + w_{1,n-1} - 2w_{1,n}) = 0 \end{aligned} \tag{5}$$

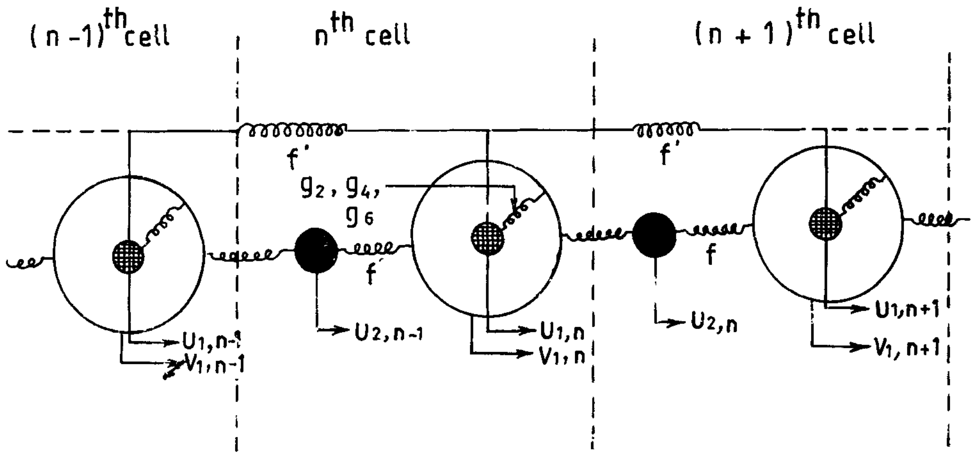

Figure 1. One-dimensional ϕ^6-polarizable model with first neighbour core-shell and core-core force constants of the anion.

with

$$\alpha = 2f + g_2, \delta = 3g_4, \gamma = 5g_6 \text{ and } 1/\mu = 1/m_2 + 2/m_1.$$

The equation of motion (5) can be solved by first considering the anharmonic oscillators as noninteracting and which are having the same mode of vibration. However, it can be solved for interacting oscillators also by considering the travelling wave type solutions for the core and shell displacements of the respective ions.

In the independent oscillator approximation (ie, $u_{1,n+1} = u_{1,n-1} = u_{1,n}$; $w_{1,n+1} = w_{1,n-1} = w_{1,n}$), the harmonic intra-site potential V_L by using the equation of motion obtained from (2) in (4) reduces to

$$V_L = \frac{g_6^2}{4f}\left[w_{1,n}^{10} + \frac{5}{4}\left(\frac{g_4}{g_6} + \frac{\delta}{\gamma}\right) w_{1,n}^8 + \frac{5}{3}\left(\frac{g_4 \delta}{g_6 \gamma} + \frac{6g_2}{\gamma}\right) w_{1,n}^6 + \frac{5}{3}\left(\frac{g_2}{g_6}\cdot\frac{2\delta}{\gamma}\right) w_{1,n}^4 + \frac{g_2^2}{g_6^2} w_{1,n}^2 \right]. \tag{6a}$$

For the first integration of (5), the equation of motions are solved by using suitable boundary conditions at the turning point w_0(i.e., at $t = 0$, $w_{1,n} = w_0$). The energy of the anharmonic oscillations at the turning point w_0 will be due to the potential (i.e., onsite and intra-site) energy of the oscillator only, as kinetic energy vanishes (since $\dot{w}_{1,n} = 0$). It can be expressed as [10]

$$E(w_0) = \frac{g_6^2}{4f}\left[w_0^{10} + \frac{5}{4}\left(\frac{g_4}{g_6} + \frac{\delta}{\gamma}\right) w_0^8 + \frac{5}{3}\left(\frac{g_4 \delta}{g_6 \gamma} + \frac{g_2}{g_6} + \frac{\alpha}{\gamma}\right) w_0^6 + \frac{5}{2}\left(\frac{g_4 \alpha}{g_6 \gamma} + \frac{g_2}{g_6} + \frac{\delta}{r}\right) w_0^4 + 5\frac{g_2 \alpha}{g_6 \gamma} w_0^2 \right]. \tag{6b}$$

The above energy expression has its turning point at $w_0 = 0$, $\pm w_1$, $\pm w_2$, $\pm w_3$ and

$\pm w_4$, which are defined as

$$\pm w_1 = \left[-\frac{g_4}{2g_6}\left\{1 + \left(1 - \frac{4g_2 g_6}{g_4^2}\right)^{1/2}\right\}\right]^{1/2},$$

$$\pm w_2 = \left[-\frac{g_4}{2g_6}\left\{1 - \left(1 - \frac{4g_2 g_6}{g_4^2}\right)^{1/2}\right\}\right]^{1/2} \tag{7}$$

and

$$\pm w_3 = \left[-\frac{\beta}{2\gamma}\left\{1 + \left(1 - \frac{4\alpha\gamma}{\beta^2}\right)^{1/2}\right\}\right]^{1/2},$$

$$\pm w_4 = \left[-\frac{\beta}{2\gamma}\left\{1 - \left(1 - \frac{4\alpha\gamma}{\beta^2}\right)^{1/2}\right\}\right]^{1/2}. \tag{8}$$

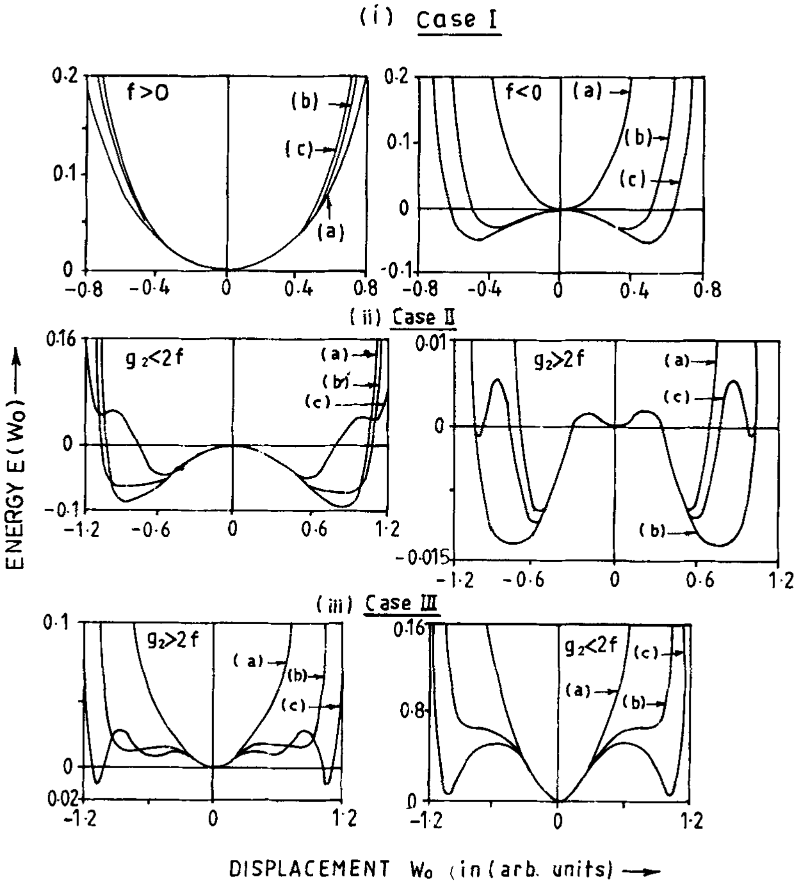

Figure 2. Energy ($E(w_0)$) (in the units of $g_6^2/4f$) versus displacement w_0 for (i) Case I ($g_2 > 0, g_4 > 0$ and $g_6 > 0$) with $f > 0$ and $f < 0$, (ii) Case II ($g_2 < 0, g_4 > 0$ and $g_6 < 0$) with $g_2 > 2f$ and $g_2 < 2f$, (iii) Case III ($g_2 > 0$, $g_4 < 0$ and $g_6 > 0$) with $g_2 > 2f$ and $g_2 < 2f$ obeying the approximations (a) $g_4^2 < 4g_2 g_6$, (b) $g_4^2 = 4g_2 g_6$ and (c) $g_4^2 > 4g_2 g_6$.

In the approximation $g_4^2 = 4g_2g_6$, the energy expression yields a triple degenerate minima corresponding to the displacements $\pm w_1$, $\pm w_2$ and $\pm w_4$ and maxima at the displacement $\pm w_3$, provided $|g_2| > 2f$. Hence the energy structure develops a harmonic potential at the origin (i.e., for small displacements) and a flattened symmetric double well for large displacements. The energy (in the units of $g_6^2/4f$) versus displacement w_0 for three different cases in the approximations $g_4^2 <, =, > 4g_2g_6$ respectively, are shown in figure 2.

However for the travelling wave solutions, ie, in the interacting oscillator mode, we have taken $g_4^2 = 4g_2g_6$, $g_2 < 0$, $g_4 > 0$, $g_6 < 0$ and $g_2 < 2f$. These conditions lead to the structural phase transition (can be seen from figure 2 (Case II(b))). In the continuum treatment we chose the solutions for the displacements in the travelling wave form as

$$u_{1,n\pm 1}\left(t \pm \frac{2a}{v}\right) = u_{1,n}(t),$$

$$u_{2,n\pm 1}\left(t \pm \frac{2a}{v}\right) = u_{2,n}(t), \tag{9}$$

where a and v are the interatomic distance and velocity of the travelling wave respectively . We make Taylor's series expansion of displacements in the travelling wave in terms of $\tau(= 2a/v)$ (similarly for $u_{2,n\pm 1}(t)$ and $w_{1,n\pm 1}(t)$) as [4]

$$u_{1,n\pm 1}(t) = u_{1,n}(t) \pm \tau \dot{u}_{1,n}(t) + \frac{\tau^2}{2}\ddot{u}_{1,n}(t). \tag{10}$$

Using (2), (9) and (10), the equation of motion (5) in the relative shell-core displacement can be expressed as

$$\left(1 + \beta - 6\beta\frac{w_{1,n}^2}{w_s^2} + 5\beta\frac{w_{1,n}^4}{w_s^4}\right)\ddot{w}_{1,n} - 12\beta w_{1,n}\frac{\dot{w}_{1,n}^2}{w_s^2}$$

$$+ 20\beta w_{1,n}^3\frac{\dot{w}_{1,n}^2}{w_s^4} + \frac{g_2}{M}w_{1,n}\left(1 - 2\frac{w_{1,n}^2}{w_s^2} + \frac{w_{1,n}^4}{w_s^4}\right) = 0, \tag{11}$$

where

$$w_s \equiv \pm\left(-\frac{g_4}{2g_6}\right)^{1/2} = \pm\left(-\frac{2g_2}{g_4}\right)^{1/2}$$

represents the minima of the ϕ^6 potential for the special case, $g_4^2 = 4g_2g_6$ (see figure 2). Here,

$$\beta = \frac{g_2}{2f}\frac{1}{\left(1 - \frac{v_2^2}{v^2}\right)}, \tag{12}$$

$$\frac{1}{M} = \frac{1}{m_1\left(1 - \frac{v_1^2}{v^2}\right)} + \frac{1}{m_2\left(1 - \frac{v_2^2}{v^2}\right)} \tag{13}$$

and

$$v_1 \equiv a\left(\frac{4f'}{m_1}\right)^{1/2}, \quad v_2 \equiv a\left(\frac{2f}{m_2}\right)^{1/2} \tag{14}$$

are the acoustic velocities near the critical temperature [2, 11]. Equation (11) contains parameters β and w_s whose values depend upon the magnitude of f, g_2 and g_4. The sign and magnitude of g_6 does not come into picture. Only the knowledge of the nature and magnitudes of f, g_2 and g_4 are needed in the calculation of dipole moment. Integrating (11) once, we obtained the equation of motion as

$$\dot{w}_{1,n}^2 = -\frac{1}{M}\left[\frac{V(w_{1,n}^4) - V(w_0^4)}{\left(1 + \beta - 6\beta\frac{w_{1,n}^2}{w_s^2} + 5\beta\frac{w_{1,n}^4}{w_s^4}\right)^2}\right], \tag{15}$$

where $\pm w_0$ are the turning points and

$$V(w_{1,n}^4) = g_2 w_{1,n}^2\left[1 + \beta - (1 + 4\beta)\frac{w_{1,n}^2}{w_s^2} + \left(\frac{1 + 18\beta}{3}\right)\frac{w_{1,n}^4}{w_s^4} - 4\beta\frac{w_{1,n}^6}{w_s^6} + \beta\frac{w_{1,n}^8}{w_s^8}\right]. \tag{16}$$

The effective potential relating the anharmonic oscillation is

$$U(w_{1,n}) = -\frac{\mu}{2M}\left[\frac{V(w_{1,n}^4) - V(w_0^4)}{\left(1 + \beta - 6\beta\frac{w_{1,n}^2}{w_s^2} + 5\beta\frac{w_{1,n}^4}{w_s^4}\right)^2}\right]. \tag{17}$$

The time period is obtained from (15) as

$$t = (-M)^{1/2}\int^{w_{1,n}} \frac{\left(1 + \beta - 6\beta\frac{w_{1,n}^2}{w_s^2} + 5\beta\frac{w_{1,n}^4}{w_s^4}\right)}{[(w_{1,n}^2 - w_0^2)\mathrm{R}(w_{1,n}^4)]^{1/2}}\,\mathrm{d}w_{1,n}, \tag{18}$$

where the lower integration limit is arbitary and

$$\mathrm{R}(w_{1,n}^4) = \frac{V(w_{1,n}^4) - V(w_0^4)}{(w_{1,n}^2 - w_0^2)} \equiv ax^4 + bx^3 + cx^2 + dx + e \tag{19}$$

is a biquadratic equation in $x (= w_{1,n}^2)$ with the coefficients

$$a = \beta\frac{g_6^2}{g_2},$$

$$b = \frac{8g_6^2\beta}{g_4} + aw_0^2,$$

$$c = \tfrac{1}{3}g_6(1 + 18\beta) + bw_0^2,$$

$$d = g_2(1 + \beta) + cw_0^2.$$

At the turning points ($\pm w_0$), $R(w_0^4)$ is factorized as

$$R(w_0^4) = g_2\left(1 - 2\frac{w_0^2}{w_s^2} + \frac{w_0^4}{w_s^4}\right)\left(1 + \beta - 6\beta\frac{w_0^2}{w_s^2} + 5\beta\frac{w_0^4}{w_s^4}\right). \tag{20}$$

Equation (18) can be solved for both periodic as well as nonperiodic solutions.

2.1 *Periodic solution*

Static periodic waves can be obtained in the limit $v \to 0$. $R(w_{1,n}^4)$ has four roots (w_1^2, w_2^2, w_3^2 and w_4^2) which can be expressed as

$$R(w_{1,n}^4) = \beta\frac{g_6^2}{g_2}(w_{1,n}^2 - w_1^2)(w_{1,n}^2 - w_2^2)(w_{1,n}^2 - w_3^2)(w_{1,n}^2 - w_4^2). \tag{21}$$

We have investigated the anharmonic periodic oscillations, in which a series representation of the integral is preferred as compared to the elliptic integral. For this purpose we assume $w_{1,n}/w_0 = \cos y$ and perform the series representation of the integral. The expression for the time period reduces to

$$t = (M)^{1/2}\int^{y}\frac{\left(1 + \beta - 6\beta\frac{w_0^2}{w_s^2} + 5\beta\frac{w_0^4}{w_s^4}\right)}{R^{1/2}(w_0^4)}\cdot\left[1 + \sum_{m=1}^{\infty} a_m \sin my\right]\mathrm{d}y, \tag{22}$$

where a_m are the coefficients of the periodic function $\sin my$. Further simplification and use of (20), reduces (22) to

$$\Omega t = -\arccos\left(\frac{w_{1,n}}{w_0}\right) - \sum_{m=1}^{\infty}\frac{a_m}{m}P_m\left(\frac{w_{1,n}}{w_0}\right), \tag{23}$$

where

$$\Omega^2 = \frac{g_2}{M}\cdot\frac{\left(1 - 2\frac{w_0^2}{w_s^2} + \frac{w_0^4}{w_s^4}\right)}{\left(1 + \beta - 6\beta\frac{w_0^2}{w_s^2} + 5\beta\frac{w_0^4}{w_s^4}\right)} \tag{24}$$

and

$$P_m\left(\frac{w_{1,n}}{w_0}\right) = 1 - \cos\left[m \arccos\left(\frac{w_{1,n}}{w_0}\right)\right]. \tag{25}$$

At the turning point w_0, the polynomial $P_m(w_{1,n}/w_0)$ vanishes. For obtaining the static periodic waves ($v \to 0$), (23) transforms into the condition

$$\Omega\tau \equiv 2ak = \left[-\frac{2g_2}{f^*}\right]^{1/2}\left(1 - 2\frac{w_0^2}{w_s^2} + \frac{w_0^4}{w_s^4}\right)^{1/2}, \tag{26}$$

where f^* is an effective force constant and is given by $f^* = 2ff'/(f + 2f')$. Periodic wave amplitude is obtained as

$$w_0^2 = w_s^2\left[1 \pm \left\{-\frac{2f^*}{g_2}a^2k^2\right\}^{1/2}\right]. \tag{27}$$

By substitution $2a^2k^2 = 1 - \cos(2ak)$ and the commensurate periodic wave condition

$2ak = 2\pi/N$, for integer N, the various wave amplitudes $w_{0,N}^2$ are obtained as

$$\begin{aligned}
w_{0,1}^2 &= w_s^2 = w_0^2,\\
w_{0,2}^2 &= w_s^2\left[1 \pm \left(-\frac{2f^*}{g_2}\right)^{1/2}\right],\\
w_{0,3}^2 &= w_s^2\left[1 \pm \left(-\frac{3f^*}{2g_2}\right)^{1/2}\right],\\
w_{0,4}^2 &= w_s^2\left[1 \pm \left(-\frac{f^*}{g_2}\right)^{1/2}\right],\\
w_{0,5}^2 &= w_s^2\left[1 \pm \left(2\left\{-\frac{f^*}{g_2}\right\}\sin^2\frac{\pi}{5}\right)^{1/2}\right],\\
w_{0,6}^2 &= w_s^2\left[1 \pm \left(-\frac{f^*}{2g_2}\right)^{1/2}\right].
\end{aligned} \tag{28}$$

Table 1. Static commensurate periodic solutions of electron-ion displacement for periods $N = 1, 2, 3, 4$ and 6.

Period $(2\pi/N)$	Electron-ion displacement $(w_{0,N})$	
	ϕ^6 model$(g_4^2 = 4g_2g_6)$	ϕ^4 model [4]
$N=1$ (ferroelectric)	$w_0^2 = -\frac{g_4}{2g_6} = -\frac{2g_2}{g_4}$	$w_0^2 = -\frac{g_2}{g_4}$
$N=2$ (antiferroelectric)	$w_0^2 = (-w_1)^2$	
	$w_0^2 = -\frac{g_4}{2g_6}\left(1 \pm \left(-\frac{4f_r}{g_2}\right)^{1/2}\right)$	$w_0^2 = -\frac{g_2}{g_4}\left(1 + \frac{4f_r}{g_2}\right)$
$N=3$ (periodon)	$w_0 = 0,\ w_1^2 = (-w_2)^2$	
	$w_1^2 = -\frac{g_4}{2g_6}\left(1 \pm \left(-\frac{3f_r}{g_2}\right)^{1/2}\right)$	$w_1^2 = -\frac{g_2}{g_4}\left(1 + \frac{3f_r}{g_2}\right)$
$N=4$	$w_0 = w_2 = 0,\ w_1^2 = (-w_3)^2$	
	$w_1^2 = -\frac{g_4}{2g_6}\left(1 \pm \left(-\frac{2f_r}{g_2}\right)^{1/2}\right)$	$w_1^2 = -\frac{g_2}{g_4}\left(1 + \frac{2f_r}{g_2}\right)$
$N=6$	$w_0 = w_3 = 0,\ w_1^2 = w_2^2 = (-w_4)^2 = (-w_5)^2$	
	$w_1^2 = -\frac{g_4}{2g_6}\left(1 \pm \left(-\frac{f_r}{g_2}\right)^{1/2}\right)$	$w_1^2 = -\frac{g_2}{g_4}\left(1 + \frac{f_r}{g_2}\right)$

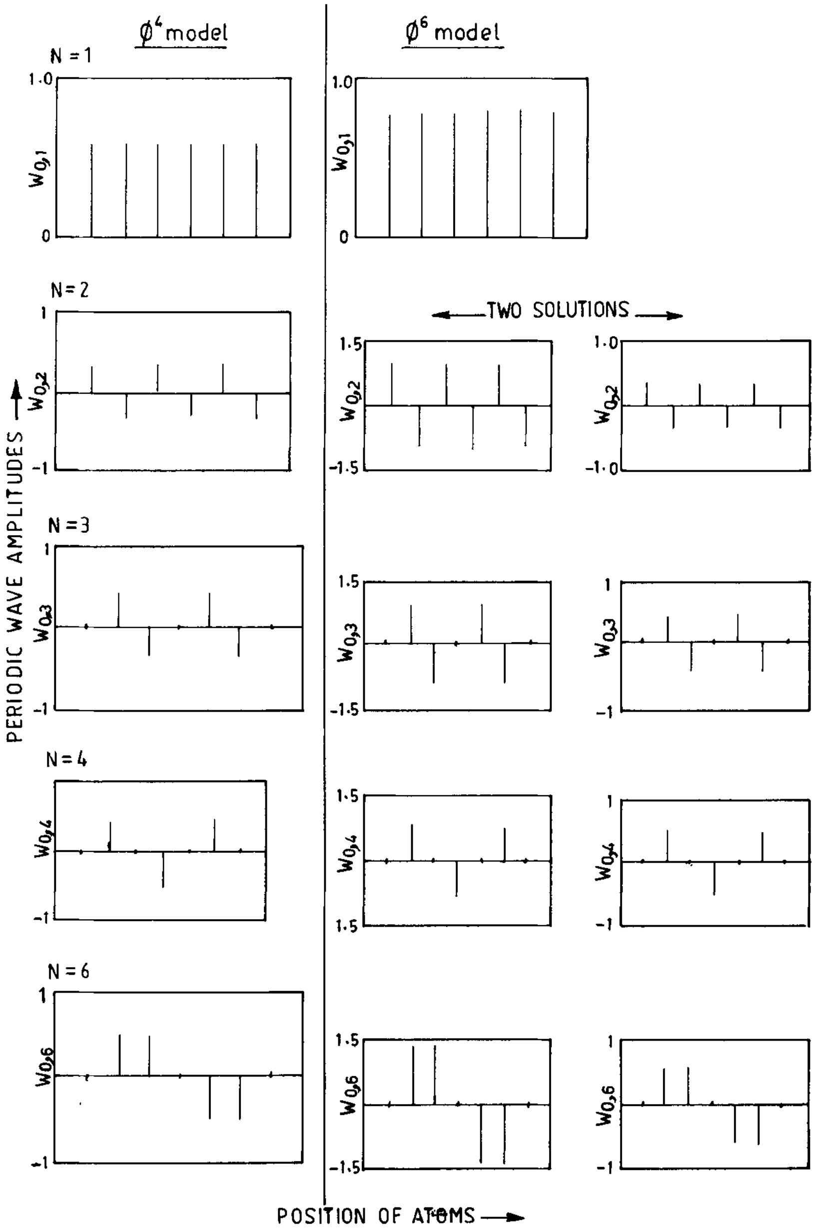

Figure 3. Displacement pattern of static commensurate periodic solutions with periods 1 to 6 for ϕ^4- and ϕ^6-polarizable models.

To have the real static periodic solutions, the value of g_2 is taken to be negative and the force constant f^* as positive. Two different trevelling periodic wave amplitudes are obtained. One travelling amplitude is always smaller than the sixth order amplitude and larger than the sixth order anti-amplitude, i.e., $w_{0,1}^2 < w_{0,N}^2 < w_{0,2}^2$, $N = 3, 4, 5, 6$.

Another travelling wave amplitude exists in the regime which is opposite in order of the previous one $[w_{0,1}^2 < w_{0,N}^2 < w_{0,2}^2]$.

Earlier, Büttner and Bilz [4] have reported the static commensurate solutions for lower order periods for a one dimensional monoatomic chain, where they have considered fourth order electron-phonon interactions at the polarizable ion. Based on the similar model treatment [4], we have calculated the electron-ion displacements for a monoatomic chain with an on-site sixth order electron-phonon coupling, by using the formula

$$w_{n+1} = \frac{1}{f_r}(g_2 w_n + g_4 w_n^3 + g_6 w_n^5) + 2w_n - w_{n-1}, \tag{29}$$

where

$$\frac{1}{f_r} = \frac{1}{f} + \frac{1}{f'}.$$

It has been found that the results obtained from (28) (ie for the sixth order periodic amplitude for a diatomic chain) are identical to the monoatomic case from eq. (26), where the effective force constant f_r corresponds to $f^*/2$. The static commensurate solutions with period 1 to 6 for ϕ^6-polarizable model are given in table 1 and comparison of our model with the ϕ^4-polarizable model are shown pictorially in terms of the relative electron-ion displacement coordinate in figure 3. $w_{0,1}$ is the amplitude of ferroelectric state which has lowest stable energy at the displacement w_s. Above these static ground states, there are nonlinear static kink-like excitations which describe the domain walls between the degenerate ground states of period $N = 2, 3, 4, 6$. As an example, the kink structure in the antiferroelectric state ($N = 2$) has sequence of the ions altered from up, down, up $\cdots$ to down, up, down $\cdots$. In the present case, we have obtained two different static periodic amplitudes, in contrast to the one obtained in ϕ^4 model results reported by Benedek [4].

2.2 *Non-periodic solutions*

Non periodic solutions are obtained if the integral of (18) diverges for some values of $w_{1,n}^2$. If one of the roots of $R(w_{1,n}^4)$ is w_0, then the expression $R(w_0^4) = 0$ yields a divergence in time. We have obtained two values of w_0^2 ie,

$$w_0^2 = w_s^2 \quad \text{or} \quad w_0^2 = w_s^2 \left\{ \frac{3}{5} \pm \frac{2}{5} \left(1 + \frac{5}{4\beta} \right)^{1/2} \right\}. \tag{30}$$

It has been found that only the first value of w_0^2 yields a divergence in time (eqs (18) and (20)). Hence the time period is obtained at $w_0^2 = w_s^2$ as

$$\Omega_s t = \int^y \frac{1 + \frac{4}{3} A_s (1 - \frac{3}{2} y + \frac{5}{4} y^2)}{(1-y)^{1/2} y^{1/2} (y-1)[1 + A_s(1 - y + y^2)]^{1/2}} \cdot \mathrm{d}y, \tag{31}$$

where

$$y = \frac{w_{1,n}^2}{w_s^2},$$

$$A_s = \frac{3\beta}{(1-3\beta)} = -\left(\frac{3g_2}{2f}\right) \cdot \left[\frac{v_2}{\left(v_2^2 - \left(1 - \frac{3g_2}{2f}\right) v^2 \right)} \right] \tag{32}$$

and

$$\Omega_s = \left[\frac{4g_2}{3M}\frac{1}{(1-3\beta)}\right]^{1/2}. \tag{33}$$

The effective potential $U(w_{1,n})$ at $w_0^2 = w_s^2$ is given by

$$U(w_{1,n}) = \tfrac{1}{2}\mu w_s^2 \Omega_s^2 \frac{(y-1)^3(1 + A_s(1-y+y^2))}{[1+\frac{4}{3}A_s(1-\frac{3}{2}y+\frac{5}{4}y^2)]^2}. \tag{34}$$

The maxima of the potential $U(w_{1,n})$ lies at $w_0^2 = w_s^2$ (i.e., $y = 1$). The derivative $dt/dw_{1,n}$ has an integrable divergence for the displacement

$$w_{1,n} = \pm\frac{w_s}{2^{1/2}}\left[1 \pm \left(1 - \frac{4}{3\beta}\right)^{1/2}\right]^{1/2} \tag{35}$$

provided $\beta \geqslant 4/3$ and $\beta < 0$.

The displacement $w_{1,n}$ can be expressed in terms of the defined parameter, A_s as

$$w_{1,n} = \pm\frac{w_s}{2^{1/2}}\left[1 \pm \left(1 - 4\left(1 + \frac{1}{A_s}\right)\right)^{1/2}\right]^{1/2} \tag{36}$$

with $A_s < 0$. We have categorized the non-periodic solutions into four groups, such as

(1) static and slowly propagating solutions,
(2) large velocity solutions,
(3) pulse solutions,
(4) fast kink and antikink solutions.

2.2.1 *Static and slowly propagating solutions*: The static ($v = 0$) and slowly propagating (for small v) travelling wave solutions exist in between two turning points, $\pm w_s$ for which, A_s is negative. These solutions are travelling kinks obeying the necessary

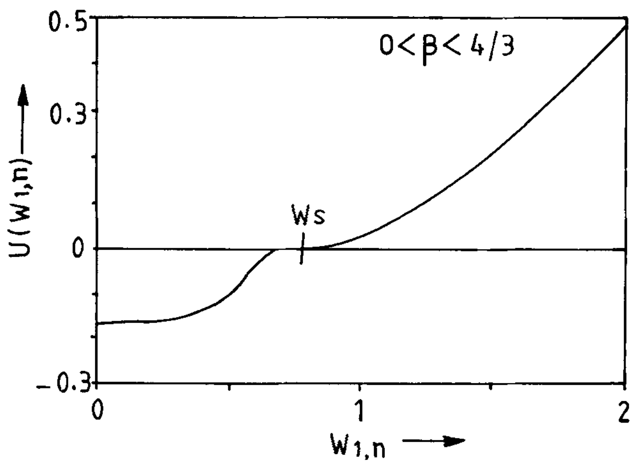

Figure 4. Effective potential $U(w_{1,n})$ as a function of core-shell displacement $w_{1,n}$ for $0 < \beta < \frac{4}{3}$.

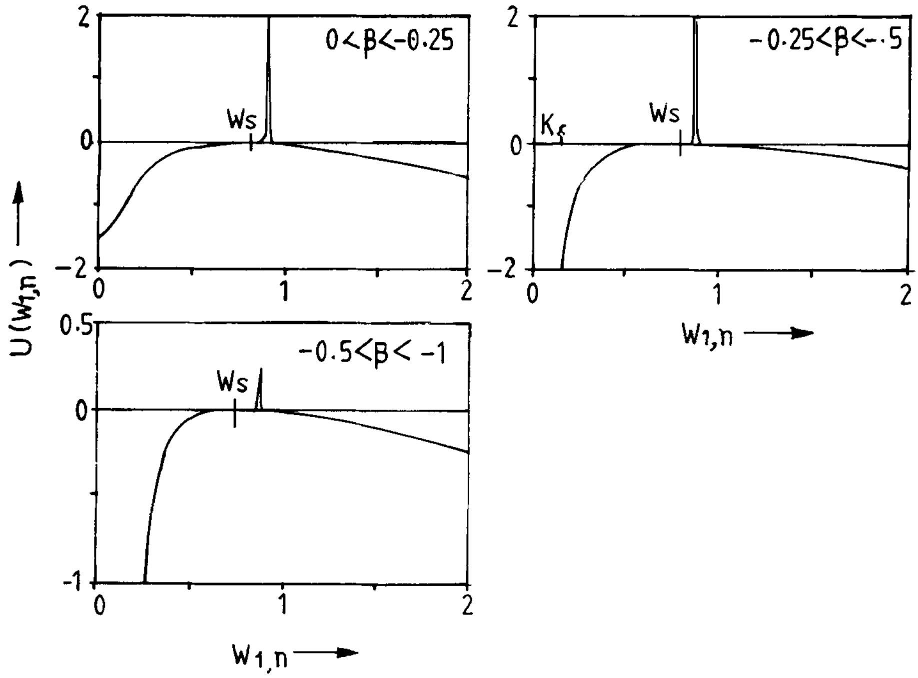

Figure 5. Effective potential $U(w_{1,n})$ as a function of core-shell displacement $w_{1,n}$ for (a) $0<\beta<-0{\cdot}25$, (b) $-0{\cdot}25<\beta<-0{\cdot}5$ and (c) $-0{\cdot}5<\beta<-1$. K_f denotes fast kinks.

condition

$$v^2 < \frac{v_2^2}{(1-2\gamma_{\phi_6})}, \tag{37}$$

with $\gamma_{\phi_6} = 3g_2/4f$. It is seen from figure 4, that for slowly moving solutions, no turning point is encountered in between $w_{1,n} = \pm w_s$, for the values of the velocity parameter $0<\beta<\frac{4}{3}$. Turning points are also obtained in the regime $w_{1,n} > w_s$ which are very close to w_s. The necessary condition for the mass ratio m_1/m_2 in the regime $0<\beta<\frac{1}{3}$ is

$$\frac{m_1}{m_2} < \frac{2f'}{f}(1+\gamma_s), \tag{38}$$

with $\gamma_s \equiv -3g_2/2f^*$.

In this regime, no consequence of the sixth order polarization potential is observed. From (34) it can be seen that the effective potential becomes infinite for the displacements

$$w_{1,n} = \pm w_s\left[\frac{3}{5}\left(1 \pm \left(1 - \frac{5}{9}\left(4 + \frac{3}{A_s}\right)\right)^{1/2}\right)\right]^{1/2}. \tag{39}$$

For $\beta>0$, the potential does not exhibit any discontinuity with respect to the displacement. The discontinuity can, however be obtained for $\beta<0$ which are also

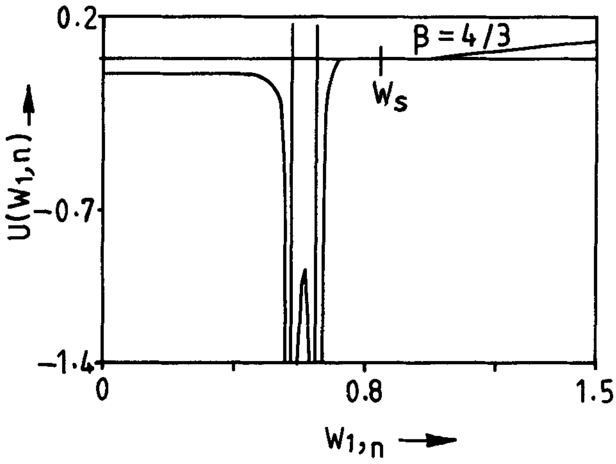

Figure 6. Effective potential $U(w_{1,n})$ as a function of core-shell displacement $w_{1,n}$ for $\beta = 4/3$.

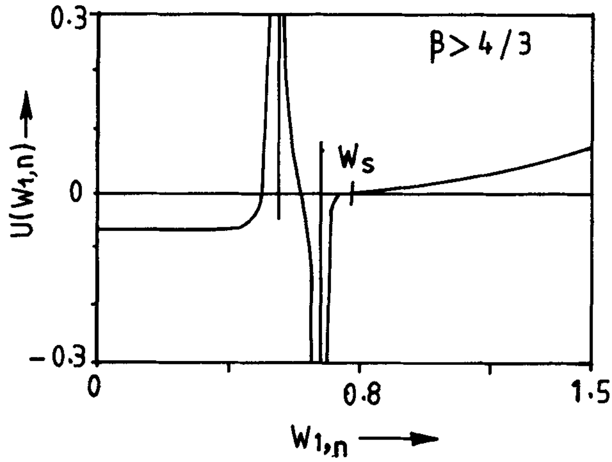

Figure 7. Effective potential $U(w_{1,n})$ as a function of core-shell displacement $w_{1,n}$ for $\beta > 4/3$. E denotes the presence of excitons.

travelling kinks obeying the condition

$$0 < v^2 < \frac{v_2^2}{(1 - 2\gamma'_{\phi_6})} \quad \text{and} \quad \frac{m_1}{m_2} < \frac{2f'}{f}(1 + \gamma'_s) \tag{40}$$

with $\gamma'_{\phi_6} \equiv -g_2/4f$ and $\gamma'_s = g_2/2f^*$. It can be noted from figure 5 that no turning point is encountered in between $w_{1,n} = 0$ and $\pm w_s$. The existence of real turning points in the regime $w_{1,n}^2 > w_s^2$ shows the presence of pulse solutions which start from the ground state polarization and returns back to the same state. Such pulse solutions are known as travelling excitons. Thus, when the velocity, $v^2 = v_2^2(1/(1 - 2\gamma_{\phi_6}))$ decreases to

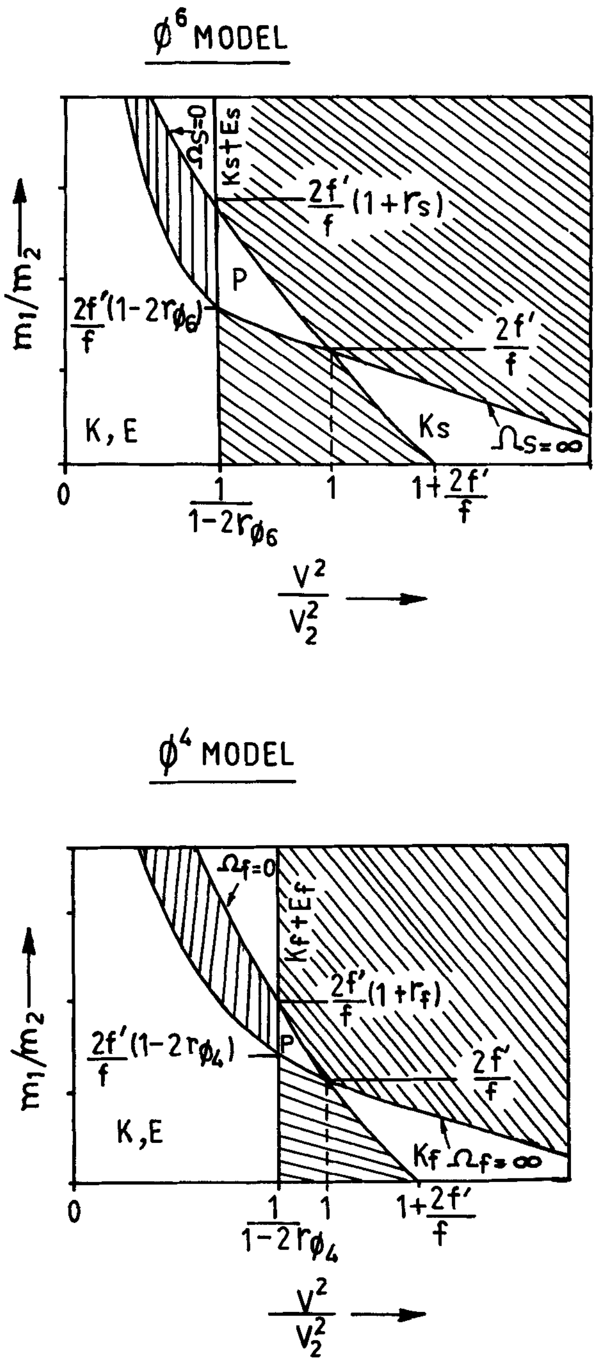

Figure 8. Ratio m_1/m_2 as a function of v^2/v_2^2 in which white areas are represented as an existence domain for (a) ϕ^4 model and (b) ϕ^6 model.

Table 2. The mass ratio m_1/m_2 as a function of velocity ratio v^2/v_2^2. Following values are plotted in figure 8.

v^2/v_2^2	Values of m_1/m_2			
	ϕ^6 model	ϕ^4 model	ϕ^6 model	ϕ^4 model
	$\Omega_s=0$ ϕ^6	$\Omega_f=0$ ϕ^4	$\Omega_s=\infty$ ϕ^6	$\Omega_f=\infty$ ϕ^4
0	∞	∞	∞	∞
$\frac{1}{(1-2\gamma_{\phi_{4,6}})}$	$\frac{2f'}{f}\frac{1}{(1+\gamma_s)}$	$\frac{2f'}{f}\frac{1}{(1+\gamma_f)}$	$\frac{2f'}{f}\frac{1}{(1-2\gamma_{\phi_6})}$	$\frac{2f'}{f}\frac{1}{(1-2\gamma_{\phi_4})}$
$\gamma_{\phi_4}=\frac{g_2}{2f}$	$\gamma_s=-\frac{3g_2}{2f^*}$	$\gamma_f=-\frac{g_2}{f^*}$		
$\gamma_{\phi_6}=\frac{3g_2}{4f}$				
1	$\frac{2f'}{f}$	$\frac{2f'}{f}$	$\frac{2f'}{f}$	$\frac{2f'}{f}$
$1+\frac{2f'}{f}$	0	0	$\frac{2f'}{(f+2f')}$	$\frac{2f'}{(f+2f')}$
∞	0	0	0	0

$v_2^2(1/(1-2\gamma'_{\phi_6}))$, some excitations are associated with the equilibrium state which can be termed as travelling excitons.

2.2.2 *Large velocity solutions*: If the velocity of the travelling wave is increased through the conditions of mass ratio, $m_1/m_2 > (2f'/f)(1+\gamma_s)$ and velocity parameter $\beta \geqslant \frac{4}{3}$, fast kinks and pulse excitons are obtained. The travelling kinks are fast because their velocity v is larger than $v_1((1+\gamma)/(1-2\gamma_{\phi_6}))^{1/2}$. When $\beta=\frac{4}{3}$ and $v^2 = \pm v_2^2(1/(1-(\gamma_{\phi_6}/2)))$, the effective potential becomes infinite for two displacements in the same direction, in between $0 < w_{1,n} < w_s$ (figure 6). As the value of β increases from 4/3, two discontinuities are obtained in the opposite direction of the potential $U(w_{1,n})$. Therefore in ϕ^6-polarizable model there exists fast travelling kinks, excitons and antikinks, as shown in figures 6 and 7.

If the velocity of the travelling wave approaches the value $\pm v_2(1+2\gamma'_{\phi_6})^{-1/2}$ then one discontinuity in $U(w_{1,n})$ is obtained near the origin (see figure 5) and another at $w_{1,n} > w_s$ provided that the mass ratio $m_1/m_2 > (2f'/f)(1+\gamma_s)$.

2.2.3 *Pulse solutions*: For the velocity lying in the range $v_2^2/(1-2\gamma_{\phi_6}) < v^2 < v_2^2(1+2f'/f)$, no kink solution is obtained. Only excitons with pulse wave behaviour exist in a restricted domain of the mass ratio $2f'/f \leqslant m_1/m_2 \leqslant (2f'/f)(1+\gamma_s)$. The parameter Ω_s decides the convergence and divergence of the time period. In the ϕ^4 model [4]

Ω_f serves the purpose ($\Omega_f = 2g_2/(M(1-2\beta))^{1/2}$). Various values of m_1/m_2 as a function of v^2/v_2^2 are given in table 2 and plotted in figure 8. It can be noted that the width of the restricted domain in ϕ^6 model is more than the ϕ^4 model.

2.2.4 *Fast kink solutions*: For the velocity of the travelling wave lying in the range $v \geqslant v_2$ and mass parameter $m_1/m_2 < 2f'/f$, fast kink solutions are obtained. Analysis of the kink solutions in the two regimes, $\beta < 0$ and $\beta > 0$, can be carried out from (31). The complete integral in (31) can be reduced in the form of elliptic integrals of first, second and third kind (given in Appendix 1).

a) $\beta < 0$: The complete analytical expression for the time period is obtained by integrating (31), where the lower limit is taken to be 1/2. The result is

$$\Omega_s t = -\frac{2(A_s+2)(8A_s+3)}{3(3A_s+4)^{1/2}}\Pi(\mu,1,q) - \frac{(21+8A_s)A_s}{3(3A_s+4)^{1/2}}F(\mu,q)$$
$$+\frac{5}{6}A_s\frac{(3A_s+4)^{1/2}}{(1+A_s)}E(\mu,q) - \left[\frac{((A_s+2)(8A_s+3)-10A_s y)}{6(1+A_s)^{1/2}}\right.$$
$$\left.\times\left(\frac{1-y}{y}+\frac{y}{1-y}+\frac{A_s+2}{A_s+1}\right)^{1/2}\right] + \frac{(3+4A_s)(3A_s+4)^{1/2}}{3}$$
$$-\frac{5}{3}(-A_s)^{1/2}\log\left[\frac{2y^{1/2}(1-y)^{1/2}\left(1+\left(1-\frac{2(A_s+1)}{A_s y(1-y)}\right)^{1/2}\right)}{\left(1+\left(-\frac{(3A_s+4)}{A_s}\right)^{1/2}\right)}\right] \tag{41}$$

with $y = w_{1,n}^2/w_s^2$, and $E(\mu,q)$, $F(\mu,q)$ and $\Pi(\mu,1,q)$ are the elliptic integrals of first, second and third kind and are expressed as

$$E(\mu,q) = \left(1-\frac{q^2}{4}-\frac{3q^4}{64}\right)\mu + \left[\sin\mu\cos\mu\left(\frac{q^2}{4}+\frac{3q^4}{64}+\frac{q^4}{32}\sin^2\mu\right.\right.$$
$$\left.\left.-\left(\frac{8}{15}\right)\left(\frac{172797}{64}\right)q^4\sin^4\mu\right)\right], \tag{42}$$

$$F(\mu,q) = \left(1+\frac{q^2}{4}+\frac{9q^4}{64}\right)\mu - \left[\sin\mu\cos\mu\left(\frac{q^2}{4}+\frac{9q^4}{64}+\frac{3q^4}{64}\sin^2\mu\right.\right.$$
$$\left.\left.-\left(\frac{8}{15}\right)\cdot\frac{518391}{64}q^4\sin^4\mu\right)\right], \tag{43}$$

$$\Pi(\mu,1,q) = I_1\left(1-\frac{q^2}{2}+\frac{3q^4}{8}\right) - \cos\mu\sin\mu\left(\frac{3q^4}{8}\right) + \mu\left(\frac{q^2}{2}+\frac{3}{16}q^4\right)$$
$$-\mu\left(\frac{3}{8}\right)q^4, \tag{44}$$

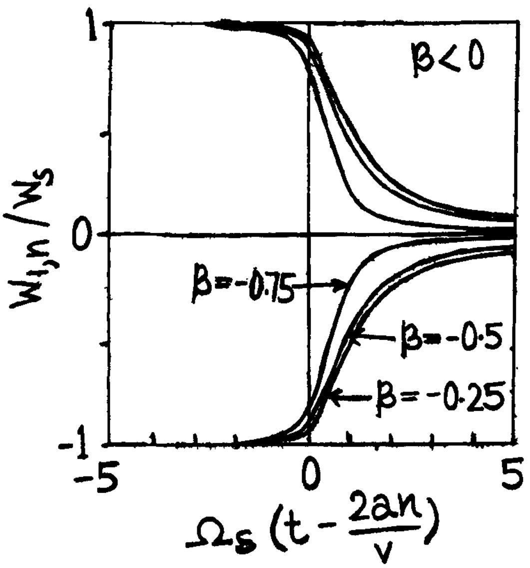

Figure 9. $w_{1,n}/w_s$ plotted as a function of $\Omega_s(t-(2an/v))$ for $\beta<0$.

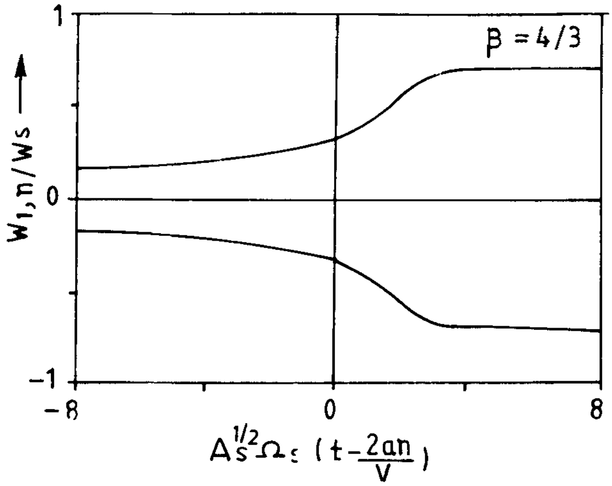

Figure 10. $w_{1,n}/w_s$ plotted as a function of $A_s^{1/2}\,\Omega_s\,(t-(2an/v))$ for $\beta=\frac{4}{3}$.

with

$$I_1=\left(1-\frac{1}{2}+\frac{3}{8}+\frac{15}{48}\right)\tan^{-1}(\sin\mu)+\sin\mu\left(\frac{1}{2}+\frac{1}{8}\sin^2\mu+\frac{3}{48}\right)\sin^4\mu$$
$$-\sin\mu\left(\frac{3}{8}+\frac{15}{48}\right), \tag{45}$$

where $q^2=-A_s/(3A_s+4)$ and $\mu=\arcsin(1-2y)$.

Exact kink and antikink solutions are obtained from (41) and are shown in figure 9 in which $w_{1,n}/w_s$ are plotted as a function of $\Omega_s(t-2an/v)$ for various values of $\beta(<0)$.

It is seen from figure 5 that the potential becomes infinite near the origin for $\beta<0$. In figure 9, kinks and antikinks are obtained in the ϕ^6 model in the regimes $-1<w_{1,n}/w_s<0$ and $0<w_{1,n}/w_s<1$, respectively. The abscissa argument $(t-2an/v)$ has been conveniently multiplied by Ω_s which decides the divergence and convergence of the travelling wave at $\pm w_s$ and 0. In the ϕ^4 treatment, only exact kink solutions are obtained in the limit $w_{1,n}/w_s=-1$ to 1 for various values of A_f (i.e. $2\beta/(1-2\beta)$) [4]. However using the ϕ^6-polarization potential, we have obtained divergence in time at the origin, in addition to $w_{1,n}/w_s=\pm 1$, which is in contrast to the behaviour in the ϕ^4-model.

b) $\beta>0$: For $\beta=\frac{4}{3}$ the expression for the time period is modified as

$$
\begin{aligned}
A_s^{1/2}\Omega_s t = {} & \frac{(6+19A_s+8A_s^2)(A_s+2)(3A_s+4)}{12(A_s+1)^2}\Pi(\mu,1,q) \\
& + \left[\frac{(12+17A_s+8A_s^2)}{3}+\frac{5}{3}\frac{(3A_s+4)A_s}{(A_s+1)}\right]F(\mu,q) \\
& + \frac{5}{6}\frac{A_s^2}{(1+A_s)}E(\mu,q)+\frac{5}{6}\frac{A_s^{3/2}}{(1+A_s)^{1/2}(1-2y)} \\
& \times\left[\frac{1-\left(\frac{A_s}{A_s+1}\right)y+\left(\frac{A_s}{A_s+1}\right)y^2}{2y(1-y)}\right]^{1/2} \\
& - \frac{(3+7A_s+4A_s^2)}{3}\left(\frac{A_s}{(1+A_s)}\right)^{1/2}\left(\frac{1-y}{y}+\frac{y}{1-y}+\frac{A_s+2}{A_s+1}\right) \\
& - \frac{5}{3}A_s\left(\cos^{-1}\left(\frac{A_s y(1-y)}{(A_s+1)}\right)^{1/2}\right),
\end{aligned}
\tag{46}
$$

where

$$\mu=\arcsin\frac{\left(1-\left(\frac{A_s}{A_s+1}\right)y+\left(\frac{A_s}{A_s+1}\right)y^2\right)^{1/2}}{(1-2y)}$$

and

$$q=2\left(\frac{A_s+1}{A_s}\right)^{1/2}.$$

In figure 10, we have plotted $w_{1,n}/w_s$ as a function of $A_s^{1/2}\Omega_s(t-2an/v)$. In this case the kink and antikink solutions are obtained in the opposite direction in the regimes $-0{\cdot}75<w_{1,n}/w_s<0{\cdot}75$.

(c) $\beta=0$(*static limit*): The expression for the time period for slow solutions (i.e., $v\to 0$) takes a simpler form, since A_s in this case is a small quantity. The slowly moving kink describing the motion of the domain along the diatomic chain is approximately

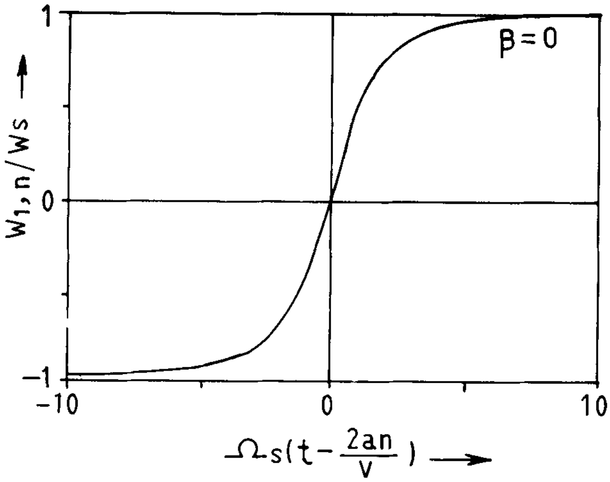

Figure 11. $w_{1,n}/w_s$ plotted as a function of $\Omega_s(t-(2an/v))$ for $\beta = 0$

given by

$$w_{1,n} = \left[-\frac{g_4}{2g_6}\right]^{1/2} \sin\left(\arctan\left(\frac{1}{2}\Omega_s\left(t-\frac{2an}{v}\right)\right)\right), \tag{47}$$

$$u_{1,n} = -\frac{4g_2}{3m_1}\frac{1}{\Omega_s^2}w_{1,n}, \tag{48}$$

$$u_{2,n} = \frac{2g_2}{3m_2}\frac{1}{\Omega_s^2}(w_{1,n}+w_{1,n-1}). \tag{49}$$

The variation of $w_{1,n}/w_s$ as a function of $\Omega_s(t-(2an/v))$ is shown in figure 11. The shape of the static ($\Omega_s \to 0$) domain wall with the value of $\Omega_s \sim \frac{2}{3}\gamma_s^{1/2}v/a$ is obtained as

$$w_{1,n} = \left[-\frac{g_4}{2g_6}\right]^{1/2} \sin(\arc\tan\tfrac{2}{3}\gamma_s^{1/2}n), \tag{50}$$

$$u_{1,n} = \frac{w_{1,n}}{\left(1+\frac{2f'}{f}\right)}, \tag{51}$$

$$u_{2,n} = \frac{(w_{1,n}+w_{1,n-1})}{\left(1+\frac{f}{2f'}\right)}, \tag{52}$$

where the width of the static domain wall is given by

$$2\left(\frac{3}{2\gamma_s^{1/2}}\right) = 2\left(-\frac{3f^*}{2g_2}\right)^{1/2} = 2\left(\frac{3f^*}{g_4}\right)^{1/2}\frac{1}{w_s} = 2\left(-\frac{3f^*}{2g_6}\right)^{1/2}\frac{1}{w_s}. \tag{53}$$

Table 3. Parameters for calculating the dipole moment per unit charge of $SrTiO_3$.

Parameters	Value [12]
$m_1(10^{-22}\text{g})$	1·549
$m_2(10^{-22}\text{g})$	1·461
$f(10^4\,\text{g/s}^2)$	14·405
$f'(10^4\,\text{g/s}^2)$	1·268
$g_2(10^4\,\text{g/s}^2)$	−2·629
$g_4(10^{22}\,\text{g/cm}^2\text{s}^2)$	0·904
$g_6(10^{40}\,\text{cm}^4\text{s}^2)$	−0·086
β	0·00025
v/v_2	0·3

As the velocity of the travelling wave increases from static value to v_1 or $v_2/((1-2\gamma_{\phi_6})^{1/2})$, the width of the moving kink decreases from the static value (eq. (53)) to zero. The width of the moving kink as a function of v is given by

$$\Gamma_s = 2\cdot\frac{3}{2}\frac{\left(1-\frac{v^2}{v_1^2}\right)^{1/2}\left(1-\frac{v^2}{v_2^2}(1-2\gamma_{\phi_6})\right)^{1/2}}{\left(1-\frac{v^2}{v_0^2}\right)^{1/2}}\cdot\frac{1}{\gamma_s^{1/2}}, \tag{54}$$

where

$$v_0 = \frac{a(2f+4f')}{(m_1+m_2)^{1/2}} \tag{55}$$

is the transverse sound velocity. As far as the size of the static domain is concerned, it has been found that the width of the static domain in ϕ^6-polarizable model is 1·225 times larger than that of the ϕ^4 model.

The various nonlinear excitations obtained in the regimes $\beta >, < 0$ are found to carry large amount of energy as compared to ϕ^4 model. The total dipole moment per unit charge of the system is

$$p_s = \frac{vw_s}{2a}\cdot\frac{1}{\Omega_s}\int\frac{w_{1,n}}{w_s}\mathrm{d}\xi, \tag{56}$$

where ξ is a dimensionless variable and can be taken as $(2a/v)\Omega_s\,(w_{1,n}/w_s)$. It is very difficult to obtain the exact analytical expression for $w_{1,n}/w_s$ as a function of $(\Omega_s t)$ for $\beta < 0$ (eq. (41)) and $(A_s^{1/2}\Omega_s t)$ for $\beta > \frac{4}{3}$ (eq. (46)), as the equations (41) and (46) are complicated.

For $SrTiO_3$, Bilz *et al* [2] have calculated the ratio v/v_2 ($v_2 \equiv a(2f/m_2)^{1/2}$) to be equal to 0·3. This value has been obtained by fitting the parameters to the experimental phonon frequencies in the self-consistent phonon approximation [2]. The parameter β is obtained by using the values of g_2, f and v/v_2 in (12). In the present ϕ^6-polarization model, for $SrTiO_3$, the model parameters (m_1, m_2, f, f', g_2 and g_4) are taken from [12] shown in table 3. These parameters are obtained by fitting the experimental data [13] on the phonon dispersion curves of $SrTiO_3$. For $v/v_2 = 0{\cdot}3$, the value of β in $SrTiO_3$ obtained is 0·00025, whose value lies in the range $0 < \beta < 1/3$. For $0 < \beta < 1/3$, the solution for the time period becomes

$$\begin{aligned}\Omega_s t = &-\frac{(6+19A_s+8A_s^2)(3A_s+4)}{6(A_s+2)(A_s+1)^{1/2}}\Pi(\mu,1,q)\\&+\left(-\frac{(6+19A_s+8A_s^2)(A_s+2)^{3/2}(3A_s+4)}{12(A_s+1)^{3/2}}+\frac{(3-A_s)}{3(1+A_s)^{1/2}}\right.\\&\left.-\frac{5A_s(3A_s+4)}{12(1+A_s)^{3/2}}\right)F(\mu,q)+\frac{5\sqrt{2}A_s}{6(1+A_s)^{1/2}}E(\mu,q)\\&-\frac{5A_s(1-2y)}{6(1+A_s)^{1/2}}\left(\frac{(A_s+1)}{2y(1-y)(1+A_s-yA_s+A_s y^2)}\right)^{1/2}\\&+\frac{(3+7A_s+4A_s^2)}{3(1+A_s)^{1/2}}\left(\left(\frac{3A_s+4}{A_s+1}\right)^{1/2}-\left(\frac{1-y}{y}+\frac{y}{1-y}+\frac{A_s+2}{A_s+1}\right)^{1/2}\right)\\&-\frac{5}{3}(-A_s)^{1/2}\log\left[\frac{2y^{1/2}(1-y)^{1/2}\left(1+\left(1-\frac{2(A_s+1)}{A_s y(1-y)}\right)^{1/2}\right)}{\left(1+\left(-\frac{(3A_s+4)}{A_s}\right)^{1/2}\right)}\right].\end{aligned} \tag{57}$$

As the equation is complicated, we chose an alternative method for calculating the dipole moment. We have obtained the corresponding numerical values of $w_{1,n}/w_s$ by changing the values of $(\Omega_s t)$ in small increments from $-\infty$ to ∞. Using standard numerical integration techniques we have then computed the integral $\int w/w_s \mathrm{d}\xi$.

Benedek *et al* [4] have found that for this value of velocity ratio, the dipole moment per unit charge in the ϕ^4 model equals to 6·3 nm, which is a large value compared to the polarization induced by ordinary optical phonons. In our model treatment, the dipole moment per unit charge is obtained as 13·325 nm. Thus it is found that the polarization induced by anharmonic phonons in the ϕ^6-model carry very large amount of energy as compared to the ϕ^4-model for a particular value of the velocity parameter β.

3. Conclusion

The present diatomic linear chain model with nonlinear polarizability of sixth order predicts very interesting nonlinear features like the static periodic waves, statics and dynamics of the domain walls, kink and antikink solutions and the existence of the travelling pulse excitons. The pulse excitons are found to carry a large amount of dipole moment for specific relative core-shell displacement, at which the potential energy becomes maximum. We have extended the treatment of Benedek *et al* [4], in which they have considered the nonlinear polarizability of the order four.

We have presented a complete analysis of the travelling wave solutions in a diatomic lattice, in the continuum limit for an anharmonic sixth order polarization potential

(ϕ^6). We have also investigated the periodic and nonperiodic solutions in the limit $g_4^2 = 4g_2g_6$. As compared to the ϕ^4 model [4], we have obtained two types of periodic travelling wave solutions. The sixth order periodic wave amplitudes are found to be identical with the amplitudes obtained in the monoatomic chain with an on-site polarizable potential of sixth order. Regarding nonperiodic solutions, we have obtained kink, antikink and excitons, depending upon different values of the mass ratio and velocity parameter. In our analysis, we have estimated the dipole moment per unit charge for $SrTiO_3$ for a standard value of velocity ratio v/v_2.

The present analytical treatment of the travelling wave solutions can be applied to the study of structural phase transition induced nonlinear dynamical excitations in many biological systems like α-double helix, optical modes of DNA and the materials having hydrogen bonded networks. The cooperative biological phenomena are caused due to the coherent excitations of the nonlinear polar modes in the form of ferroelectric groups. This type of study will help in understanding the nature of many phenomena like transport of ions, energy and the polarization inside biological membranes [14].

Appendix 1

$$
\begin{aligned}
\Omega_s t &= \left(1+\frac{4A_s}{3}\right)\int_{1/2}^{y}\left[\frac{1}{(1-y)^{1/2}y^{1/2}(y-1)(1+A_s(1-y+y^2))^{1/2}}\right]\mathrm{d}y \\
&\quad -2A_s\int_{1/2}^{y}\left[\frac{y^{1/2}}{(1-y)^{1/2}(y-1)(1+A_s(1-y+y^2))^{1/2}}\right]\mathrm{d}y \\
&\quad +\frac{5}{3}A_s\int_{1/2}^{y}\left[\frac{y^{3/2}}{(1-y)^{1/2}(y-1)(1+A_s(1-y+y^2))^{1/2}}\right]\mathrm{d}y \\
&= \frac{(6+19A_s+8A_s^2)}{6\sqrt{2}(1+A_s)^{1/2}}\int_{1}^{z}\frac{z\mathrm{d}z}{(z-1)^{1/2}(z+1)^{1/2}\left(z+\dfrac{(A_s+2)}{2(A_s+1)}\right)^{1/2}} \\
&\quad +\frac{(3-A_s)}{3\sqrt{2}(1+A_s)^{1/2}}\int_{1}^{z}\frac{\mathrm{d}z}{(z-1)^{1/2}(z+1)^{1/2}\left(z+\dfrac{(A_s+2)}{2(A_s+1)}\right)^{1/2}} \\
&\quad -\frac{5A_s}{6\sqrt{2}(1+A_s)^{1/2}}\int_{1}^{z}\frac{(z-1)^{1/2}\mathrm{d}z}{(z+1)^{1/2}\left(z+\dfrac{(A_s+2)}{2(A_s+1)}\right)^{1/2}} \\
&\quad +\frac{(3+7A_s+4A_s^2)}{3(1+A_s)^{1/2}}\left[\left(\frac{3A_s+4}{A_s+1}\right)^{1/2}-\left(\frac{(1-y)}{y}+\frac{y}{(1-y)}+\frac{A_s+2}{A_s+1}\right)^{1/2}\right] \\
&\quad +\frac{5A_s}{6\sqrt{2}(1+A_s)^{1/2}}\int_{1}^{z}\frac{\mathrm{d}z}{(z+1)\left(z+\dfrac{(A_s+2)}{2(A_s+1)}\right)^{1/2}},
\end{aligned}
\tag{A1}
$$

since $z = \frac{1}{2}[((1-y)/y) + y/(1-y)]$.

The first three integrals in (A1) are known as elliptic integrals. The expression can be reduced to square roots of third and fourth degree polynomial and their products with rational functions

$$\mu = \arcsin\left(\frac{u-a}{u-b}\right)^{1/2} \quad \text{and} \quad q = \left(\frac{b-c}{a-c}\right)^{1/2}$$

for the integral

$$\int_{\alpha}^{u} \frac{dz}{(z-a)^{1/2}(z-b)^{1/2}(z-c)^{1/2}} = \frac{2}{(a-c)^{1/2}} F(\mu, q) \qquad [u > a > b > c],$$

$$\int_{\alpha}^{u} \frac{z dz}{(z-a)^{1/2}(z-b)^{1/2}(z-c)^{1/2}} = \frac{2}{b(a-c)^{1/2}} [a(a-\mathrm{b})\Pi(\mu, 1, q) + b^2 F(\mu, q)] \qquad [u > a > b > c],$$

$$\int_{\alpha}^{u} \frac{(z-a)^{1/2} dz}{(z-b)^{1/2}(z-c)^{1/2}} = -2(a-c)^{1/2} E(\mu, q) + 2\left[\frac{(u-a)(u-c)}{(u-b)}\right]^{1/2} \qquad [u > a > b > c].$$

$E(\mu, q)$, $F(\mu, q)$ and $\Pi(\mu, 1, q)$ are the elliptic integrals of first, second and third kind. For $\beta < 0$: $a = 1, b = -1, c = -(A_s + 2)/2(A_s + 1), u = z$; $\beta \geqslant 4/3$: $a = -(A_s + 2)/2(A_s + 1)$, $b = 1, c = -1, u = z$; and $0 < \beta < \frac{1}{3}$: $a = 1, b = -(A_s + 2)/2(A_s + 1), c = -1, u = z$.

The last term in (A1) has its value as

$$-\frac{5}{3} A_s \left(\cos^{-1}\left(\frac{A_s y(1-y)}{(A_s + 1)}\right)^{1/2} - \cos^{-1} 1\right) \quad \text{for } \beta = 4/3$$

and

$$-\frac{5}{3}(-A_s)^{1/2} \log\left[\frac{2y^{1/2}(1-y)^{1/2}\left(1 + \left(1 - \frac{2(A_s+1)}{A_s y(1-y)}\right)^{1/2}\right)}{\left(1 + \left(-\frac{(3A_s+4)}{A_s}\right)^{1/2}\right)}\right]$$

for $\beta < 0$ and $0 < \beta < 1/3$.

Acknowledgements

Authors acknowledge the work of A Bussmann-Holder, H Bilz and H Buttner. One of the authors (NDC) acknowledges the financial support of CSIR in the form of Research Associateship. SPS is grateful to UGC for Career Award, financial assistance from UGC, CSIR, DST, New Delhi and DAE, Bombay.

References

[1] R Migoni, H Bilz and D Baurele, *Phys. Rev. Lett.* **37**, 1155 (1976)
J A Krumhansl and J R Schrieffer, *Phys. Rev.* **B11**, 3535 (1975)

[2] H Bilz, A Bussmann-Holder, G Benedek, H Buttner, D Strausch, *Ferroelectrics* **25**, 339 (1980)
H Buttner, in *Nonlinear phenomena at phase transitions and instabilities* edited by T Riste (Plenum, 1981)

[3] H Buttner and H Bilz, *J. Phys.* (*Paris*) **C6**, 111 (1981)
H Buttner and H Bilz, *Recent Developments in Condensed Matter Physics* edited by J T Devreese (Plenum Press, New York, 1981)
[4] G Benedek, A Bussmann-Holder and H Bilz, *Phys. Rev.* **B36**, 630 (1987)
[5] H Frohlich, *Int. J. Quantum Chem.* **2**, 641 (1968)
H Haken, *Synergetics* (Springer-Verlag, Heidelberg, 1978)
F Kaiser, *Z. Naturforsch.*, **A33**, 294, 418 (1978)
H Bilz, H Buttner and H Frohlich, *Z. Naturforsch.* **366**, 208 (1981)
[6] T Riste, E J Samuelson, K Otnes and J Feder, *Solid State Commun.* **9**, 1455 (1971)
S M Shapiro, J D Axe, G Shirane and T Riste, *Phys. Rev.* **B6**, 4332 (1972)
A D Bruce and R A Cowley, *Adv. Phys.* **29**, 219 (1980)
K A Muller, in *Nonlinear phenomena at phase transitions and instabilities* edited by T Riste (Plenum, New York, 1982), p. 1
K A Muller, in *Statics and dynamics of nonlinear systems* edited by G Benedek, H Bilz, R Zeyher (Springer, Heidelberg, 1983) **47**, 68
[7] S N Behera and A Khare, *Pramana – J. Phys.* **15**, 245 (1980)
[8] R Adair, L L Chase and S A Payne, *Phys. Rev.* **B39**, 3337 (1989)
[9] E Magwari, *Z. Phys.* **B43**, 345 (1981)
S N Behera and A Khare, *Pramana – J. Phys.* **15**, 245 (1980)
B Dey, *J. Phys.* **C19**, 3365 (1986)
[10] N D Chowdhury, Nonlinear dynamical theory of condensed matter, Ph.D Thesis, University of Bhopal (1993) (unpublished)
[11] A Bussmann-Holder, H Bilz and P Vogl, in *Dynamical properties of IV-VI compounds* (Springer, Berlin, 1983)
[12] A Bussmann-Holder, H Bilz and G Benedek, *Phys. Rev.* **B39**, 9214 (1989)
[13] R A Cowley, *Phys. Rev.* **134**, A981 (1964)
W G Stirling and R Currat, *J. Phys.* **C9**, L519 (1976)
W G Stirling, *J. Phys.* **5**, 2711 (1972)
[14] A J Martin, *Biopolymers* **23**, 471 (1984)